

# A Simple Constitutive Model for Ratcheting Evolution of 63Sn-37Pb Solder under Multiaxial Loading

XU CHEN<sup>1,2</sup> and DE-HUA YU<sup>1</sup>

1.—School of Chemical Engineering & Technology, Tianjin University, Tianjin 300072, People's Republic of China. 2.—E-mail: xchen@tju.edu.cn

A series of multiaxial ratcheting experiments has been conducted on 63Sn-37Pb solder alloys. It is shown that the ratcheting rate in each loading step keeps constant under constant axial stress and cyclic shear strain range. However, the ratcheting rate is sensitive to the shear strain rate. Based on the Edmunds–Beer (E–B) equation, a simple constitutive model is proposed to predict the ratcheting rate of each loading step. The results have shown that the model can predict the experimental data well.

**Key words:** Ratcheting, multiaxial loading, cyclic plasticity, constitutive model, 63Sn-37Pb solder

## INTRODUCTION

Eutectic Sn-Pb solder has been commonly used in electronic packaging for its suitable physical properties and low cost. The long-term reliability of the solder joints has always been a major concern because of the complex loading condition and severe service environment in electronic packages. Generally, the thermomechanical fatigue caused by the thermal expansion difference between the different packaging materials due to the temperature fluctuations is believed to be the main reason for packaging failure.<sup>1</sup>

In fact, the solder joints in electronic packages are often subjected to asymmetrical cyclic shear loading due to the mismatch of the thermal expansion coefficient, and multiaxial stress states will occur if an axial stress exists. Under such multiaxial loading conditions, ratcheting, which is a cyclic accumulation of plastic strain, will take place in solder joints. The ratcheting deformation can contribute to the material damage and reduce the fatigue life of solder. Although many researchers, including Chaboche and Nouailhas,<sup>2,3</sup> McDowell,<sup>4</sup> Hassan and Kyriakodes,<sup>5,6</sup> Jiang and Schitoglu,<sup>7</sup> Ohno and Wang,<sup>8,9</sup> and Chen et al.,<sup>10–13</sup> have reported experimental results of uniaxial and multiaxial ratcheting for various materials, and the art of modeling the ratcheting behavior has already made significant advances in the past two decades, studies of the ratcheting behavior of eutectic solder are rare.

Moreover, most of the ratcheting models are too complex for engineering applications, especially the models for multiaxial loading. In this study, a series of multiaxial ratcheting experiments, which have not previously been performed on eutectic solders, are conducted on 63Sn-37Pb solder, and a simple constitutive model based on the Edmunds–Beer equation is proposed to predict the ratcheting rate of each loading step.

## EXPERIMENTS

The 63Sn-37Pb specimen, which has undergone annealing treatment,<sup>14</sup> is shown in Fig. 1. The tests were conducted at room temperature on an Instron (Instron Ltd, UK) axial-torsional test machine. A clip-on tension-torsion extensometer was mounted on the outside of the specimen to measure the multiaxial deformation. All the ratcheting tests were conducted under stress control for axial loading and under strain control for torsional loading. Each test consisted of several loading steps. In each loading step, the axial load was kept at a constant value and the torsional load at various strain rates was cycled under fully reversed strain control.

The hysteresis loops in ratcheting tests under axial stress control are not closed. Therefore, the following definitions of the axial ratcheting strain and its rate in a cycle are introduced as follows:

$$\varepsilon_r = \frac{\varepsilon_{\max} + \varepsilon_{\min}}{2} \quad (1)$$

$$\dot{\varepsilon}_r = d\varepsilon_r/dN \quad (2)$$

(Received April 30, 2005; accepted August 29, 2005)

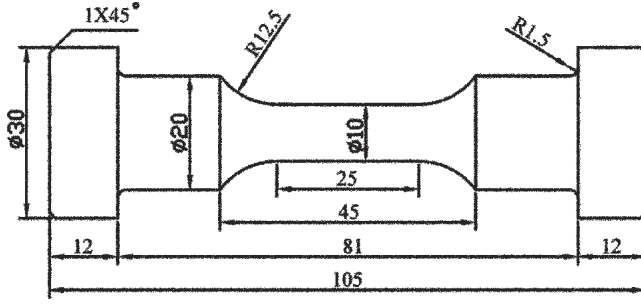


Fig. 1. Specimen geometry (millimeters).

where  $\varepsilon_{\max}$  and  $\varepsilon_{\min}$  are maximums and minimums of the axial strain in a cycle, respectively, and  $N$  is the number of cycles.

In the multiaxial ratcheting tests, the torsional cycle had constant shear strain amplitude, and the axial stress varied in several steps in each test, that is, tensile stress for odd step and compression stress for even step. The test conditions are given in Table I.

In the multiaxial ratcheting tests, the calculation of shear stress at the outer radius of a round bar specimen is not straightforward because the shear stress is nonlinearly distributed along the radius. The shear stress amplitude on the surface of the specimen under such biaxial loading conditions can be approximately determined using the following formula:

$$\tau = \frac{1}{2\pi R^3} \left[ 3T + \gamma \frac{dT}{d\gamma} \right] \quad (3)$$

where  $R$  is the specimen radius,  $T$  is the torque amplitude,  $\gamma$  is the shear strain amplitude, and  $dt/d\gamma$  is the slope of the  $T - \gamma$  hysteresis loop.

In order to get the true shear stress rather than engineering shear stress, the radius change caused by axial tension and compression must be taken into account. The real value of the radius is obtained by using the Poisson's effect relationship:

$$\frac{R - R_0}{R_0} = -\nu \varepsilon_t \quad (4)$$

where  $R_0$  is the initial radius,  $R$  is the real value,  $\varepsilon_t$  is the total axial strain, and  $\nu$  is the Poisson's ratio.

Generally, the following equation is used to estimate the value of Poisson's ratio.<sup>15</sup>

$$\nu = 0.5 - (0.5 - \nu_e) \frac{\varepsilon_e}{\varepsilon_t} \quad (5)$$

where  $\nu_e = 0.35$  is Poisson's ratio for the elastic strain. The terms  $\varepsilon_e$  and  $\varepsilon_t$  are axial elastic strain and total strain, respectively. The elastic strain can be obtained as

$$\varepsilon_e = \frac{\sigma}{E} \quad (6)$$

In this work, the maximum axial stress was controlled as 10 MPa and the Young's modulus  $E = 28,000$  MPa. Taking the loading case with the maximum axial stress as an example, the Poisson's ratio calculated by Eq. 5 is 0.49866.

It is very close to the value of 0.5 for the plastic range and the error is 0.268%. Thus, the influence of elastic Poisson's ratio was neglected in this study.

Here,  $\nu_p = 0.5$  is used in consideration of large plasticity.<sup>15</sup> So the real radius in each cycle is approximately given by

$$R = R_0(1 - \nu_p \varepsilon_t) \quad (7)$$

## RESULTS AND DISCUSSION

It is found that the rate of ratcheting remains almost constant under the constant axial stress and torsional strain amplitude, i.e., the ratcheting evolution curve of each loading step is approximately linear. The axial stress and torsional strain amplitude have great influence on ratcheting rates. The ratcheting strain rate is very sensitive to the applied shear strain rate. However, loading history and loading sequence have no significant influence on ratcheting strain, as shown in Fig. 2. Steps 1, 3, and 5 are with tensile stress and steps 2, 4, and 6 are with compression stress.

The ratcheting rate of Sn-Pb solder is a function of applied axial stress, shear strain amplitude, and shear strain rate, which can be expressed as the following formula:

$$d\varepsilon_r/dN = f\left(\sigma, \frac{\Delta\gamma}{2}, \dot{\gamma}\right) \quad (8)$$

Table I. Experiment and Predicted Values

Specimen	Stage	Axial Stress $\sigma$ (MPa)	Shear Strain $\Delta\gamma/2$ (%)	Shear Strain Rate $d\gamma/dt$ (L/s)	Ratcheting Rate ( $10^{-4}/\text{cycle}$ )	
					Experiment	Prediction
SN21	Step 1	10	0.866	$1.7 \times 10^{-3}$	11.98	$\pm 11.0$
	Step 2	-10	0.866		-13.52	
	Step 3	10	0.52	$1 \times 10^{-2}$	4.65	$\pm 3.22$
	Step 4	-10	0.52		-4.76	
	Step 5	10	0.52		4.90	
SN41	Step 1	5	0.52	$1 \times 10^{-3}$	2.71	$\pm 3.23$
	Step 2	-5	0.52		-2.99	
	Step 3	5	0.52	$1 \times 10^{-2}$	1.47	$\pm 1.47$
	Step 4	-5	0.52		-1.37	
	Step 5	5	0.52	$1 \times 10^{-4}$	7.24	$\pm 7.11$
	Step 6	-5	0.52		-7.03	

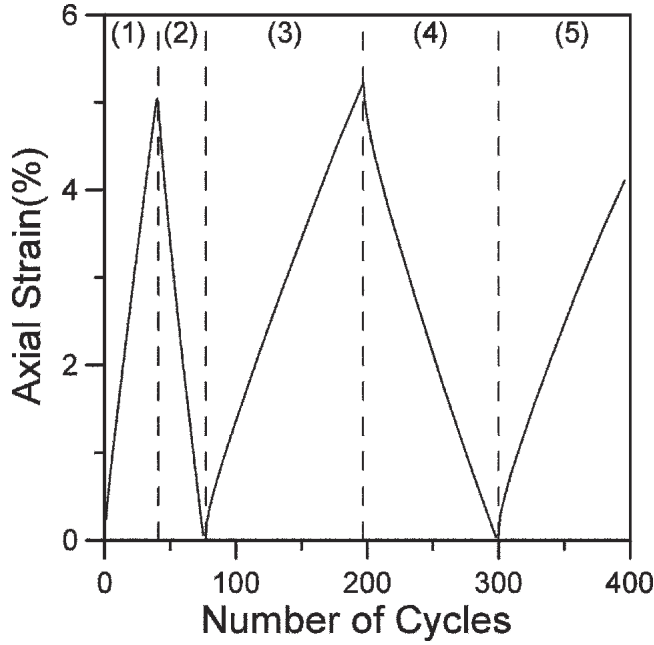


Fig. 2. Ratcheting strain with cycles for specimen SN21.

where  $d\varepsilon_r/dN$  is ratcheting strain per cycle,  $\sigma$ ,  $\Delta\gamma/2$ ,  $\dot{\gamma}$  are applied axial stress, shear strain amplitude, and shear strain rate, respectively.

Based on perfect elastic-plastic assumptions, Edmunds and Beer deduced an equation to calculate the irreversible increment of plastic strain per cycle of a rectangular plate subjected to conjugate strain cycles superimposed on constant direct stress.<sup>16</sup> The Edmunds-Beer (E-B) equation, expressed as follows, was once used to simulate the ratcheting strain rate of pressurized pipe.<sup>16,17</sup>

$$d\varepsilon_r/dN = \frac{3\sigma_h}{(2\sigma_y - \sigma_h)} \left[ 2\varepsilon_b - \frac{(2\sigma_y - \sigma_h)}{E} \right] \quad (9)$$

where  $\sigma_y$ ,  $\sigma_h$ , and  $\varepsilon_b$  were, respectively, yield stress, hoop stress, and cyclic axial bending strain. However, the E-B equation is too conservative and overestimates the ratcheting strain in pressurized pipe.<sup>16</sup> It also overestimates the ratcheting rate of Sn-Pb solder. More importantly, the equation cannot predict the rate-dependent ratcheting of solder. Therefore, the E-B equation should be modified in order to obtain more accurate results. In the presence of the E-B equation, a simple model with a rate function, which takes account of the rate-dependent ratcheting characteristic, is proposed as follows:

$$d\varepsilon_r/dN = \text{sgn} \cdot \frac{3\sigma}{(2\sigma_y - |\sigma|)} \cdot \left[ 2 \left( \frac{\Delta\gamma}{2} \right) - \frac{(2\sigma_y - |\sigma|)}{E} \right] \cdot f(\dot{\gamma}) \quad (10)$$

where  $|\sigma|$  is the absolute value of axial stress,  $\sigma_y$  is yield stress,  $E$  is the Young's modulus,  $f(\dot{\gamma})$  is a function of the shear strain rate effect, and  $\dot{\gamma}$  is the shear strain rate. Here,  $E = 28,000$  MPa is obtained

through monotonic tension experiments at room temperature. For Sn-Pb solder, there is no obvious yield point before fracture. The yield stress is defined as  $\sigma_y = \sigma_{0.2} = 40$  MPa, and  $\text{sgn}$  is used to determine the direction of the ratcheting strain. When axial stress is positive (tension), the axial ratcheting strain evolves in tension and the value of  $\text{sgn}$  is set as +1; on the contrary, when axial stress is negative (compression), the value of  $\text{sgn}$  is -1.

Based on the multiaxial ratcheting experiment results at different shear strain rates, it is found that the shear strain rate effect is an exponential function, as shown in Fig. 3. The function can be fitted as

$$f(\dot{\gamma}) = 0.0196(\dot{\gamma})^{-0.3427} \quad (11)$$

As shown in Table I and Fig. 4, the E-B equation overestimates the ratcheting strain and cannot describe the rate-dependent ratcheting behavior, but the modified Eq. 10 can predict with much accuracy the ratcheting rate for different shear strain rates. Without many complex coefficients to determine, the simple model is promising to be easily used in engineering applications.

Creep deformation can occur in solder at room temperature because of its low melting point. The axial mean stress in ratcheting tests may induce creep deformation. The creep strain needs to be subtracted from the ratcheting strain to evaluate the ratcheting rate correctly. An axial creep test was conducted on a specimen at the same axial stress level as that of SN41. The creep strain was found to be less than 0.5% during the test duration, as shown in Fig. 5, and the creep strain rate was rather small, except at the beginning where primary creep prevails. Compared with ratcheting strain at the same duration, the axial creep strain rate is negligible. Thus, the axial strain rate under cyclic torsional

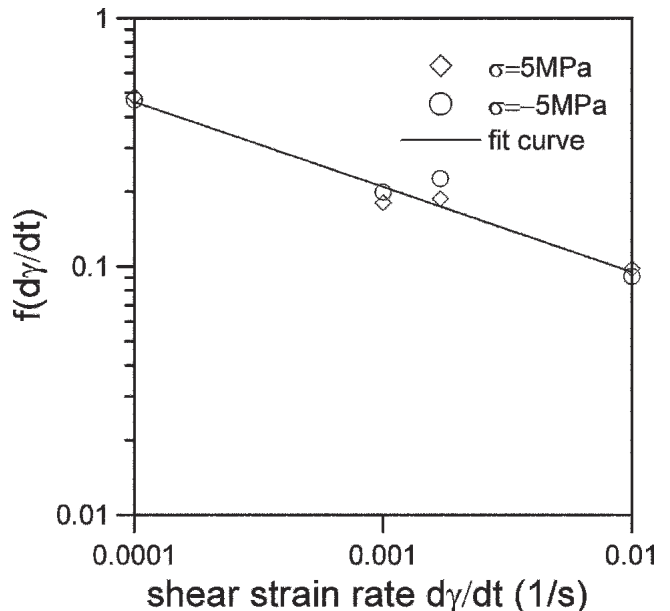
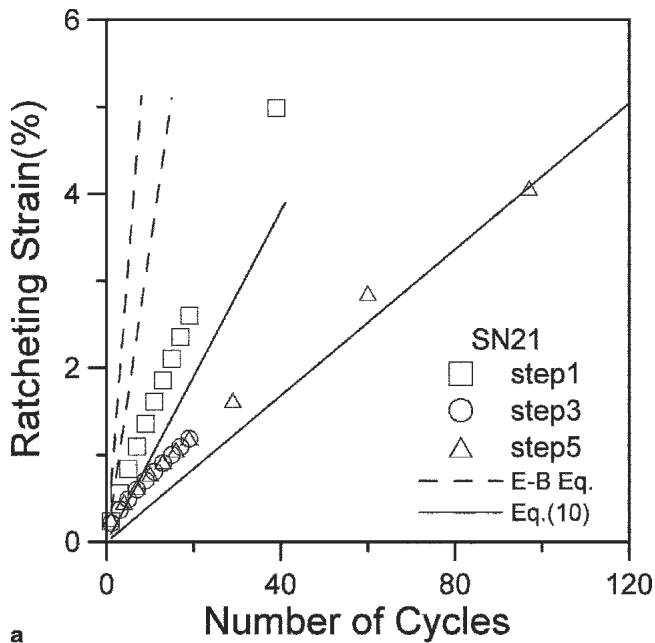
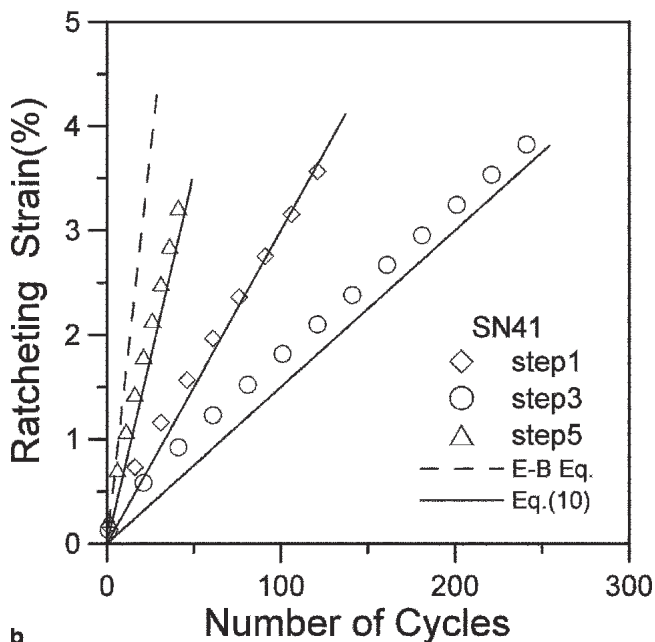


Fig. 3. The relationship between strain rate coefficient and shear strain rate.



a



b

Fig. 4. Comparison of predictions and experiments for ratcheting strain: (a) SN21 specimen and (b) SN41 specimen.

loading may be considered approximately as the ratcheting strain rate.

As shown in Fig. 4, the ratcheting rates predicted from Eq. 10 are constant and the ratcheting evolution curves are linear. Therefore, for the materials whose ratcheting rates decay rapidly (e.g., medium carbon steel<sup>11</sup>), the model will not present good predictions.

### CONCLUSIONS

The ratcheting rate of Sn-Pb solder is a function of applied axial stress, shear strain amplitude, and shear strain rate. The E-B equation overestimates the ratcheting rate of solder and cannot describe the

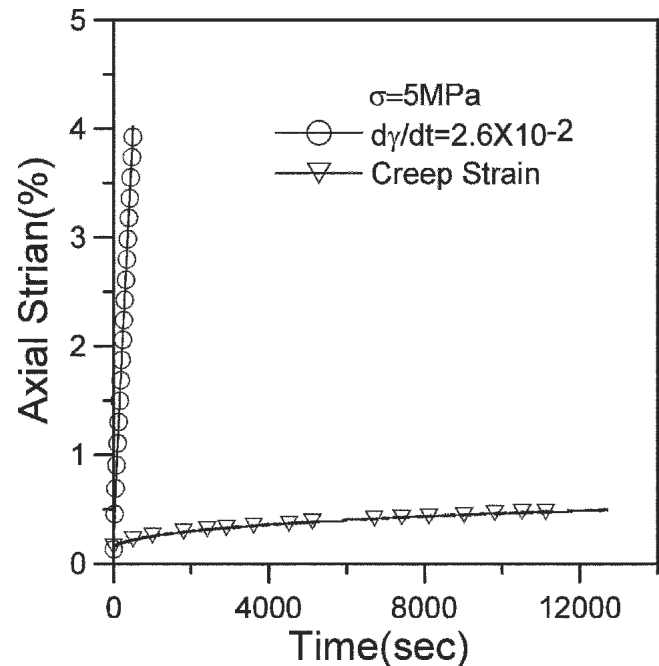


Fig. 5. Axial ratcheting strain and axial creep strain with time.

rate-dependent ratcheting behavior. A modified model, which accounts for the rate-dependent ratcheting behavior of Sn-Pb solder, is proposed to predict the ratcheting rate of each loading stage. The results have shown that the model can predict the experimental data well.

### ACKNOWLEDGEMENTS

The authors gratefully acknowledge the financial support for this work from National Natural Science Foundation of China under Grant No. 10272080 and the Teaching and Research Award Program for Outstanding Young Teachers in Higher Education Institutions of MOE, People's Republic of China.

### REFERENCES

1. X.Q. Shi, H.L.J. Pang, W. Zhou, and Z.P. Wang, *Int. J. Fatigue* 22, 217 (2000).
2. J.L. Chaboche and D. Nouailhas, *ASME Trans. J. Eng. Mater. Technol.* 111, 384 (1989).
3. J.L. Chaboche and D. Nouailhas, *ASME Trans. J. Eng. Mater. Technol.* 111, 409 (1989).
4. D.L. McDowell, *Eur. J. Mech. A/Solid* 13, 593 (1994).
5. T. Hassan and S. Kyriakodes, *Int. J. Plast.* 8, 91 (1992).
6. T. Hassan and S. Kyriakodes, *Int. J. Plast.* 8, 117 (1992).
7. Y. Jiang and H. Schitoglu, *ASME Trans. J., Appl. Mech.* 63, 720 (1996).
8. N. Ohno and J.D. Wang, *Int. J. Plast.* 9, 375 (1993).
9. N. Ohno and J.D. Wang, *Int. J. Plast.* 9, 391 (1993).
10. X. Chen and R. Jiao, *Int. J. Plast.* 20, 871 (2004).
11. X. Chen, R. Jiao, and K.S. Kim, *Int. J. Plast.* 21, 161 (2005).
12. X. Chen and K.S. Kim, *Acta Mechanica* 163, 9 (2003).
13. X. Chen, R. Jiao, and K.S. Kim, *Int. J. Solid Struct.* 40, 7449 (2003).
14. X. Chen, D. Jin, M. Sakane, and T. Yamamoto, *J. Electron. Mater.* 34, L1 (2005).
15. K. Rahka and C.J. Laird, *J. Test. Evaluation* 14, 173 (1986).
16. H.G. Edmunds and F.J. Beer, *J. Mech. Eng. Sci.* 3, 187 (1961).
17. R.J. Scavuzzo, P.C. Lam, and J.S. Gau, *ASME Trans. J. Pressure Vessel Technol.* 113, 210 (1991).